NACA

RESEARCH MEMORANDUM

MEASUREMENTS OF BOUNDARY-LAYER TRANSITION AT LOW SPEED ON TWO BODIES OF REVOLUTION IN A LOW-TURBULENCE WIND TUNNEL

By Frederick W. Boltz, George C. Kenyon,
and Clyde Q. Allen

Ames Aeronautical Laboratory
Moffett Field, Calif.

NATIONAL ADVISORY COMMITTEE
FOR AERONAUTICS

WASHINGTON
September 26, 1956

NATIONAL ADVISORY COMMITTEE FOR AERONAUTICS

RESEARCH MEMORANDUM

MEASUREMENTS OF BOUNDARY-LAYER TRANSITION AT LOW SPEED ON TWO BODIES OF REVOLUTION IN A LOW-TURBULENCE WIND TUNNEL

By Frederick W. Boltz, George C. Kenyon, and Clyde Q. Allen

SUMMARY

An investigation of the location of transition from laminar to turbulent flow in the boundary layer on two bodies of revolution at zero angle of attack has been made in a low-turbulence wind tunnel. One body was a prolate spheroid of fineness ratio 9.0 and was constructed of aluminum. The other body, a modified prolate spheroid of fineness ratio 7.5 was constructed of steel and covered with Fiberglas and resin. Both bodies were instrumented with subsurface microphones to detect the location of transition from laminar to turbulent flow in the boundary layer.

Data are presented for a range of low speeds at a constant stagnation pressure near atmospheric. These data include transition Reynolds numbers and pressure distributions for both bodies of revolution. Also included are the theoretical boundary-layer parameters. In order to expedite publication, the data are presented without discussion.

INTRODUCTION

In recent years considerable attention has been focused on the stability of the laminar boundary layer and on various means of controlling and delaying the transition of this laminar flow to turbulent flow. While abundant data on boundary-layer transition are available for two-dimensional-flow conditions, there is considerably less information on three-dimensional bodies. Accordingly, it was decided to conduct experimental studies on the boundary layers of bodies of revolution in a low-turbulence air stream.

An investigation was undertaken in the Ames 12-foot pressure wind tunnel of the boundary-layer characteristics of two bodies of revolution having fineness ratios of 7.5 and 9.0. The location of transition on both

bodies has been determined for a range of Reynolds numbers at low speeds. In order to expedite release of the data, the results are presented without discussion.

NOTATION

c	a constant
L	body length
p	static pressure
P	static-pressure coefficient, $\frac{p_l - p_\infty}{\frac{1}{2} p_\infty U_\infty^2}$
R	Reynolds number, $\frac{U_\infty L}{\nu}$
R_{trans}	Reynolds number at transition, $\frac{U_\infty x}{\nu}$
R_{δ^*}	Reynolds number based on displacement thickness, $\frac{U_\infty \delta^*}{\nu}$
s	distance from the nose, along a meridian
U	velocity
x	axial distance along the body
β	potential-flow parameter where $U_l = cs^{\frac{\beta}{2-\beta}}$
δ^*	boundary-layer displacement thickness
θ	boundary-layer momentum thickness
ν	kinematic viscosity
ρ	air density

Subscripts

l	local
∞	free stream

MODELS AND INSTRUMENTATION

Models

Two bodies of revolution were tested during this investigation. One body was a prolate spheroid of fineness ratio 9.0, and the other body was a modified prolate spheroid of fineness ratio 7.5. Both bodies were sting-mounted at the center of the wind-tunnel test section. A comparative sketch of the two bodies is shown in figure 1.

Fineness-ratio 9.0 body.- The coordinates of this body are listed in table I and a photograph of the model is presented as figure 2. Beginning at the 92-percent station the body was faired into a 4-inch-diameter sting.

The body was fabricated of 1/4-inch-thick cast-aluminum shells which were bolted together at integral internal flanges. The polished surface was estimated to have an average surface roughness of less than 30 micro-inches, as determined by reference to roughness gages. The surface waviness was measured with a 2-1/2-inch-span surface gage and was found to be less than 0.0003 inch per inch.

Fineness-ratio 7.5 body.- The coordinates of this body are listed in table I. The rear half of the body was a prolate spheroid of fineness ratio 7.5. The forward half of the body was contoured so as to provide a favorable pressure gradient over a longer portion of the body length than could be obtained with a fineness ratio 7.5 prolate spheroid. Beginning at the 95-percent station, the body was faired into a 4-inch-diameter sting. Figure 3 is a photograph of the body.

This body differed in construction and material from the first body. It was constructed of steel shells welded together around a core of steel tubing. This shell was covered with a 1/4-inch layer of Fiberglas resin which, in turn, was coated with a 1/32-inch layer of epoxy-resin. The resin surface was sprayed with several coats of hard lacquer and hand rubbed with number 600 sandpaper to a smooth finish. The surface roughness was comparable to that of the aluminum body. The surface waviness was less than 0.0004 inch per inch, measured with a 2-1/2-inch-span surface gage.

Instrumentation

The bodies were equipped with static-pressure orifices as listed in table II. Certain orifices (see table II) were closely coupled to miniature magnetic-type receivers (U. S. Signal Corps Headset HS-30-U) which were used as microphones to detect the pressure fluctuations in the boundary layer. The output of the microphones was passed through an amplifier to a headset receiver and an oscilloscope. The amplified

microphone signal indicated the type of flow in the boundary layer. Shown in figure 4 is a photographic record of the oscilloscope trace of a typical pattern of "bursts" in the transition region, as well as the laminar and turbulent flow patterns. Since transition develops over some distance, the microphone signal in this region is characterized by more frequent turbulent bursts as the completely turbulent region is approached. To provide a uniform interpretation of the signal throughout the tests, the beginning of transition was defined as approximately two bursts per second. It should be noted that in each of the three traces shown in figure 4 there is a common waviness due to the internal "noise" of the electrical equipment.

TESTS

The investigation was conducted in the Ames 12-foot pressure wind tunnel with the model at zero angle of attack. The variations of Reynolds number were obtained by varying the velocity in the test section at a constant stagnation pressure near atmospheric pressure. As the free-stream velocity was increased, the location of transition moved progressively forward on the bodies. With transition identified at each successive microphone station, pressure, temperature, and velocity were recorded. Blockage corrections to the data were computed and found to be negligible.

Since a knowledge of the turbulence level of the air stream was desirable, measurements of the turbulence were made with a hot-wire anemometer. The anemometer was a constant-current type having a compensated amplifier. The tungsten hot-wire had a diameter of 0.00015 inch and a length of 0.105 inch. Results of the turbulence survey indicate that, at the low speeds encountered in this investigation, the longitudinal component of the velocity fluctuation was less than 0.02 percent.

RESULTS

In order to expedite publication, these data are presented without discussion. The static-pressure coefficients for the two bodies are presented in table III, and a comparison plot of these data is presented in figure 5. It should be pointed out that these pressure-coefficient values are averages obtained from a number of test runs, ranging in Mach number from 0.1 to 0.3. The maximum deviation of the measured pressure coefficients from the average values was about ±0.005.

In figure 6 the variation of transition Reynolds number with length Reynolds number is presented. The shaded areas represent the accuracy and repeatability of the experimentally determined transition Reynolds numbers. Since detailed boundary-layer measurements were not made, various laminar boundary-layer parameters were computed for the two bodies, using

the technique of Falkner and Skan (ref. 1), and are compared in figure 7. In these computations the Mangler transformation (ref. 2) from a three-dimensional body to an equivalent two-dimensional body was used.

Ames Aeronautical Laboratory
National Advisory Committee for Aeronautics
Moffett Field, Calif., July 17, 1956

REFERENCES

1. Falkner, V. M.: A Further Investigation of Solutions of the Boundary Layer Equations. R. & M. No. 1884, British A.R.C., 1937.

2. Mangler, W.: Boundary Layers on Bodies of Revolution in Symmetrical Flow. Joint Intelligence Objectives Agency, Washington, D. C., B.I.G.S. 13, 26 June 1946.

TABLE I.- BODY OF REVOLUTION COORDINATES
[All dimensions given in percent length]

Fineness ratio 9.0 body		Fineness ratio 7.5 body	
Station	Ordinate	Station	Ordinate
0	0	0	0
.5	.81	.5	.95
1.1	1.14	1.0	1.29
2.1	1.60	2.0	1.75
3.2	1.95	3.0	2.09
4.2	2.24	4.0	2.38
5.3	2.49	5.0	2.64
6.3	2.71	6.0	2.88
7.4	2.91	7.0	3.10
8.5	3.09	8.0	3.30
9.5	3.26	9.0	3.49
10.6	3.42	10.0	3.67
15.9	4.06	15.0	4.46
20.1	4.45	20.0	5.10
25.4	4.84	25.0	5.62
30.7	5.12	30.0	6.02
34.9	5.30	35.0	6.31
40.2	5.45	40.0	6.51
45.5	5.53	45.0	6.63
50.0	5.55	50.0	6.67
55.5	5.52	55.0	6.63
60.8	5.42	60.0	6.53
65.1	5.30	65.0	6.36
70.4	5.07	70.0	6.11
75.6	4.77	75.0	5.77
80.9	4.36	80.0	5.33
85.2	3.95	85.0	4.76
89.9	3.34	90.0	4.00
95.2	2.59	95.0	2.91
100.5	2.06	100.0	2.08

TABLE II.- STATIC-PRESSURE ORIFICE LOCATIONS
[All dimensions given in percent length]

Fineness ratio 9.0 body	Fineness ratio 7.5 body
Upper surface meridian	Upper surface meridian
Station	Station
5.8	0
11.5	.20
20.8	.59
28.6[a]	1.50
34.3[a]	2.95
45.3[a]	4.80
54.1[a]	7.10
63.5[a]	9.95[a]
70.8[a]	15.00[a]
77.1[a]	20.00[a]
81.7[a]	24.92[a]
85.9[a]	30.00[a]
91.6[a]	35.00[a]
	40.00[a]
	45.00[a]
	49.98[a]
	55.00[a]
	60.00[a]
	65.00[a]
	70.00[a]
	75.00[a]
	80.00[a]
	85.00[a]
	90.00[a]

[a]Denotes microphone at orifice station.

TABLE III.- STATIC-PRESSURE DISTRIBUTION
[All dimensions given in percent length]

Fineness ratio 9.0 body		Fineness ratio 7.5 body	
Station	P	Station	P
5.8	-0.006	0.59	0.283
11.5	-.030	1.50	.101
20.8	-.040	2.95	.051
28.6	-.044	4.80	.026
34.3	-.046	7.10	.010
45.3	-.048	9.95	-.006
54.1	-.050	15.00	-.030
63.5	-.046	20.00	-.051
70.8	-.042	24.92	-.067
77.1	-.034	30.00	-.073
81.7	-.020	35.00	-.077
85.9	-.004	40.00	-.080
91.6	.069	45.00	-.080
		49.98	-.074
		55.00	-.071
		60.00	-.069
		65.00	-.067
		70.00	-.065
		75.00	-.061
		80.00	-.053
		85.00	-.032
		90.00	0
		100.00	.182

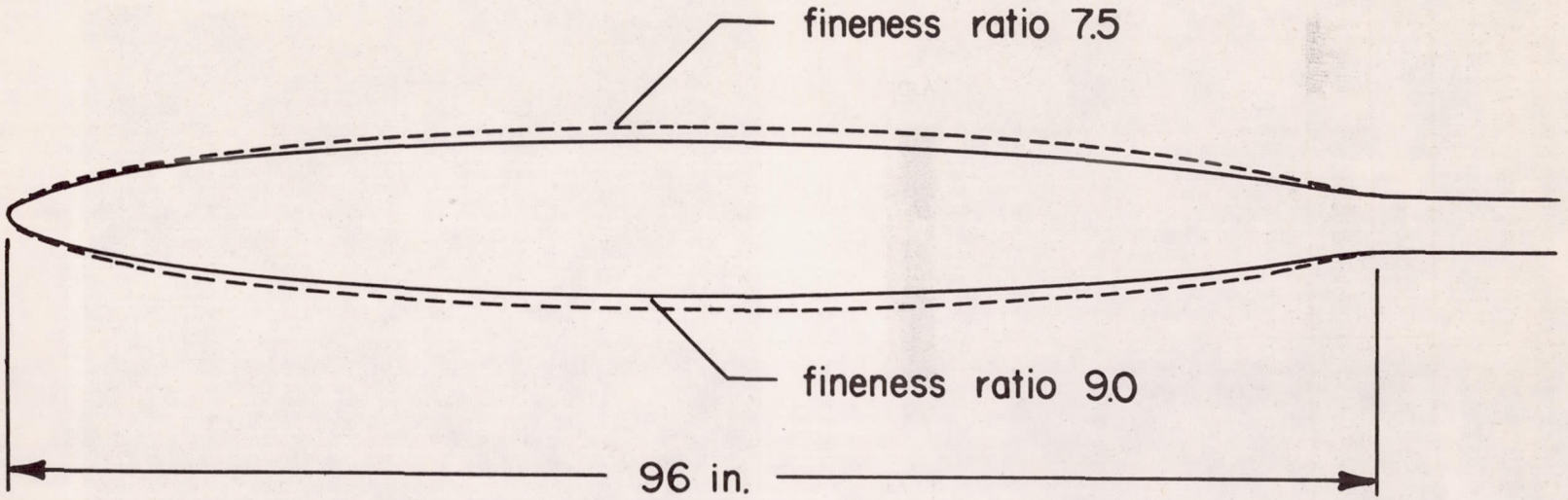

Figure 1.- A comparison of the profiles of the bodies.

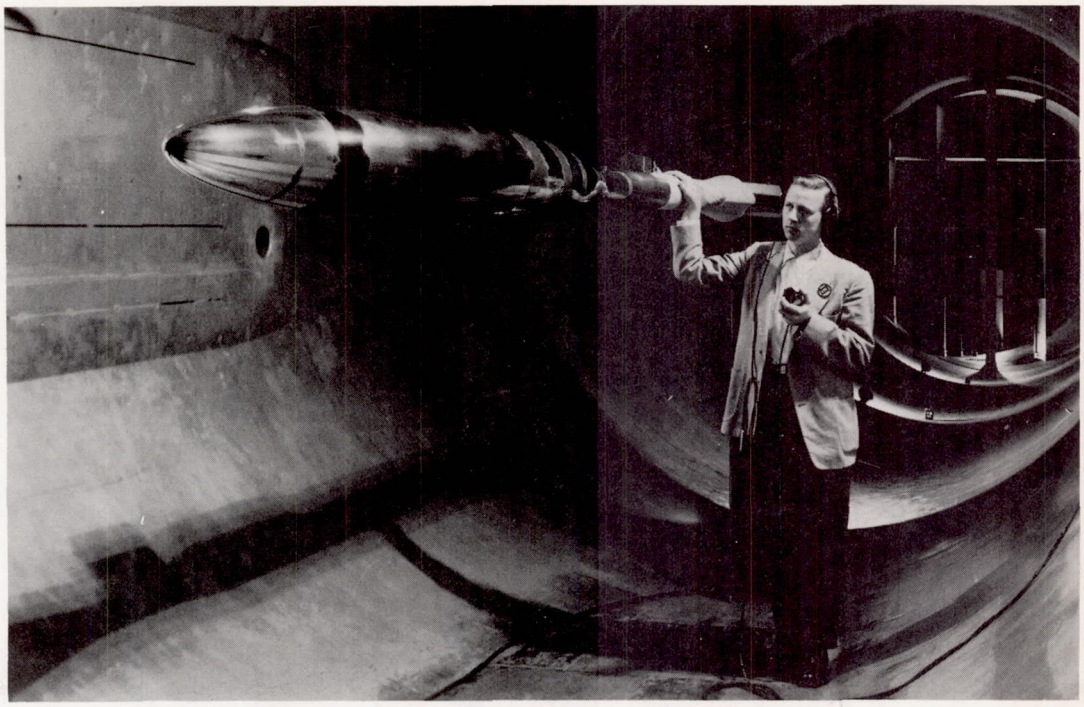

A-19928.1

Figure 2.- The body of fineness ratio 9.0 mounted in the test section.

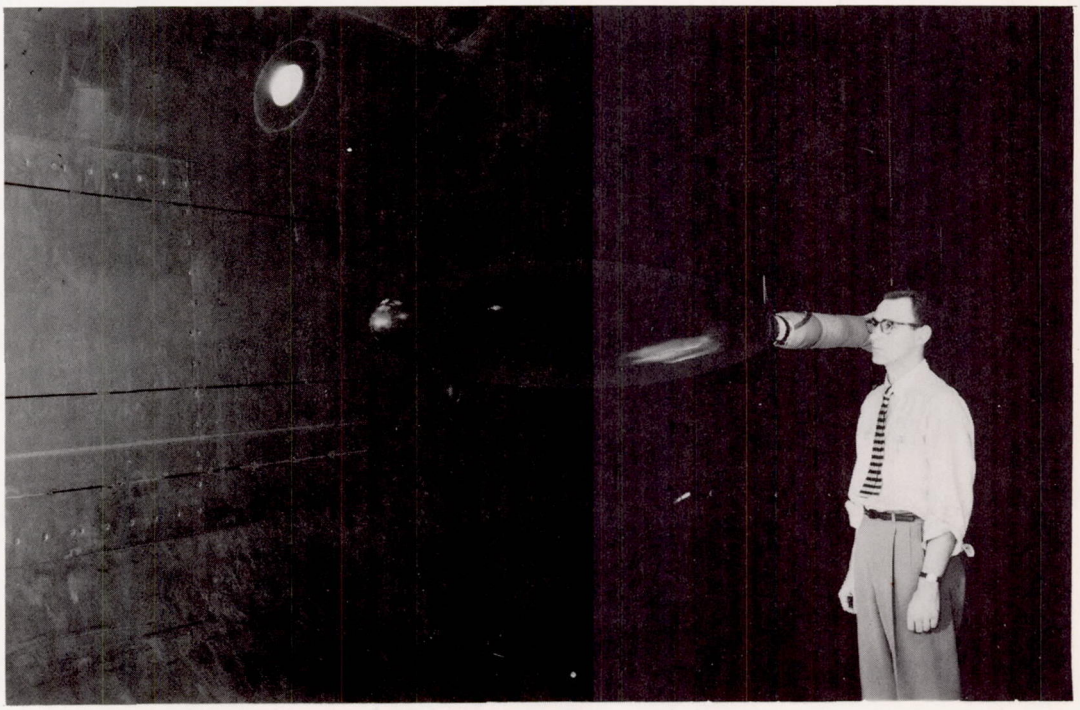

A-21104.1

Figure 3.- The body of fineness ratio 7.5 mounted in the test section.

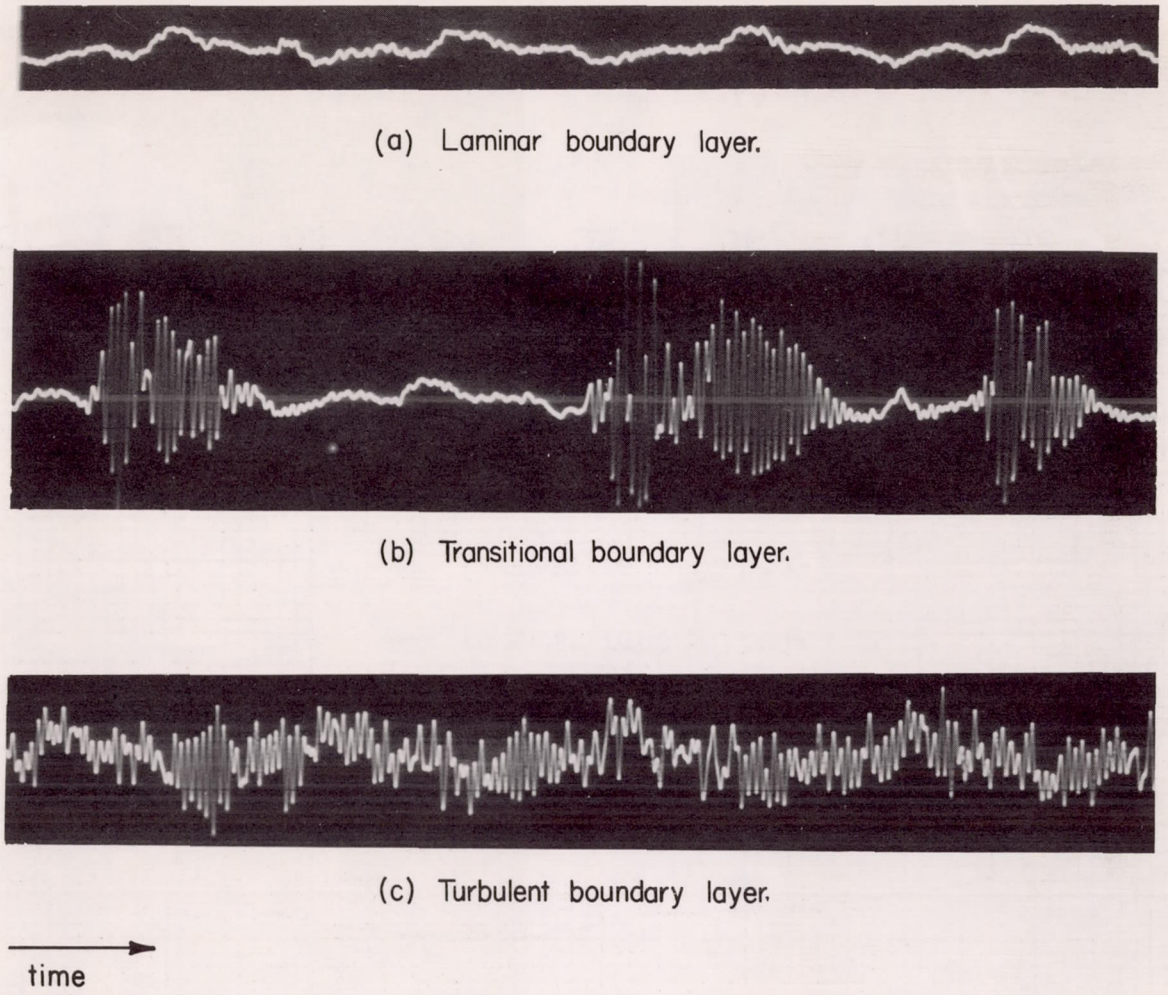

Figure 4.- Oscilloscope traces of the microphone response for the three types of boundary layers.

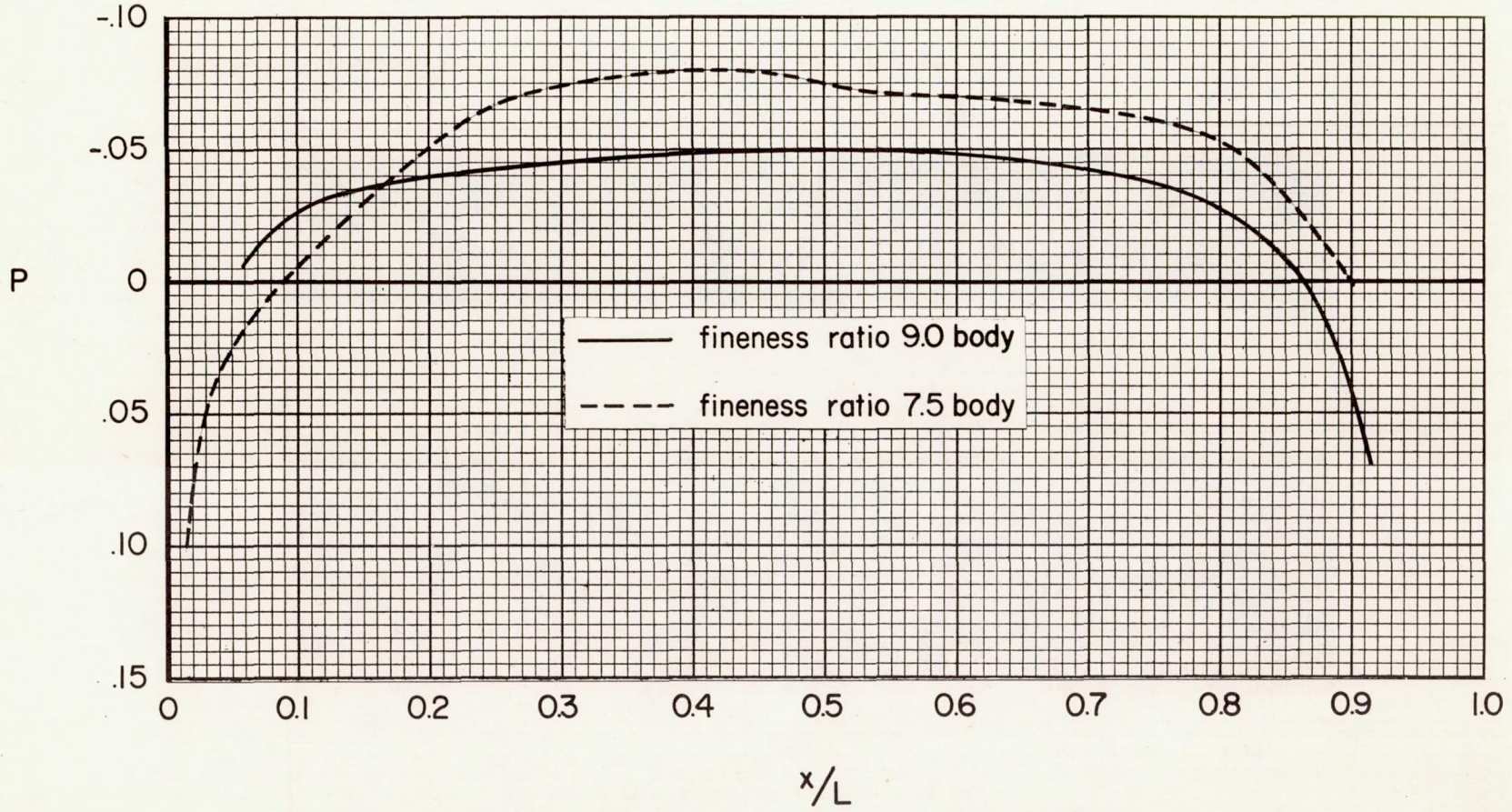

Figure 5.- The static-pressure distribution on the bodies.

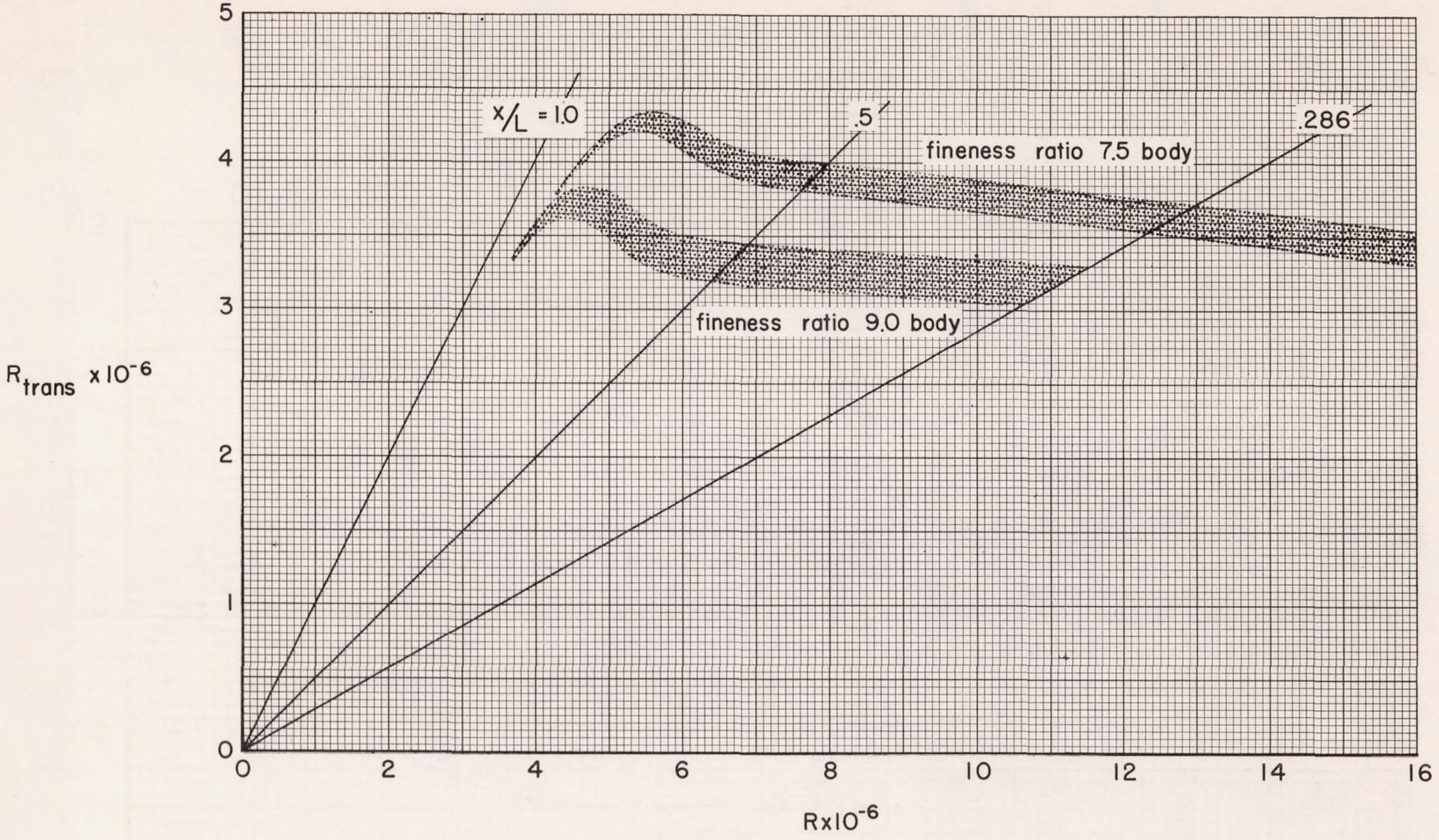

Figure 6.- The variation of transition Reynolds number with length Reynolds number for the bodies.

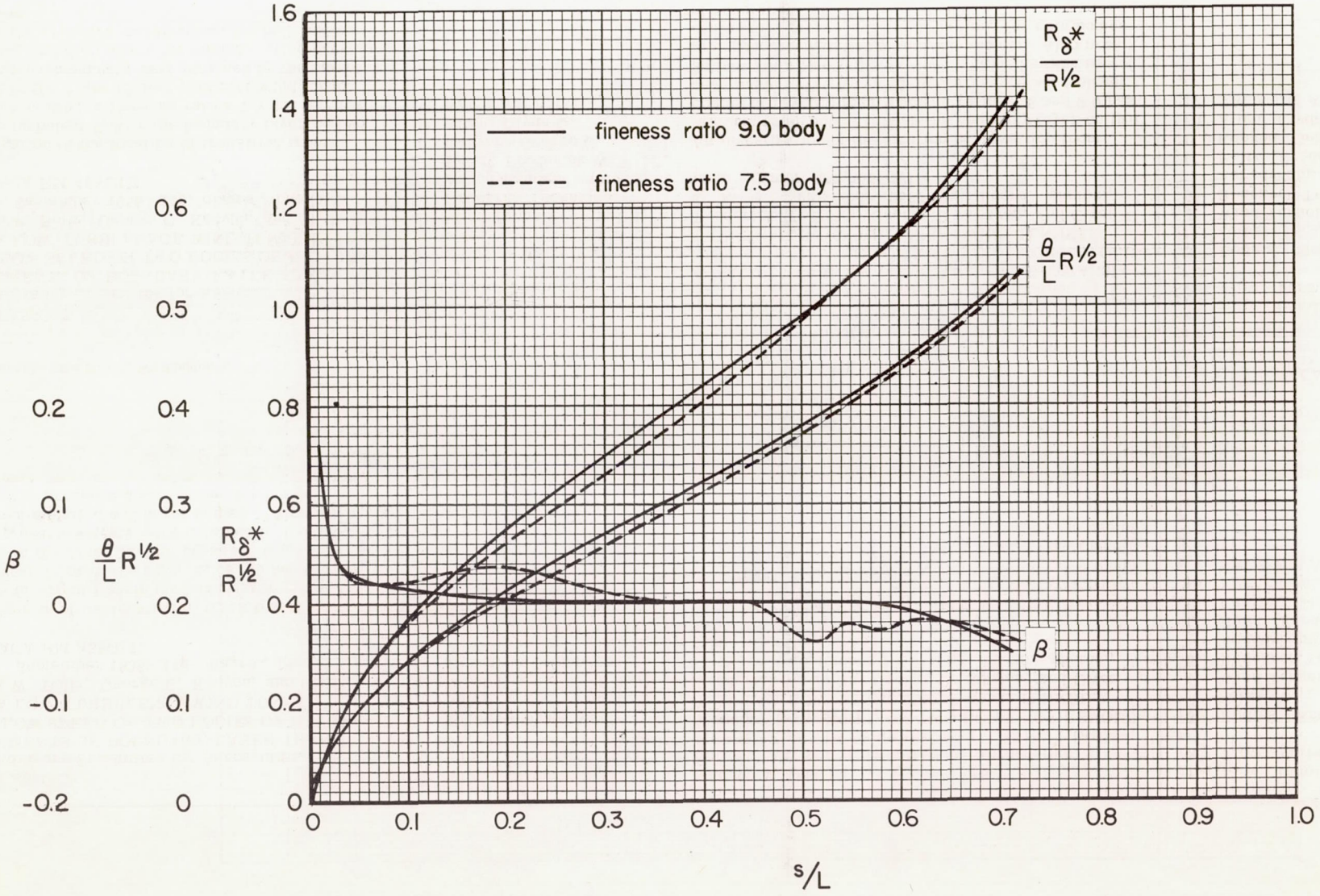

Figure 7.- Computed laminar boundary-layer characteristics of the bodies.